Electronic Supplementary Material (ESI) for Energy & Environmental Science.
This journal is © The Royal Society of Chemistry 2024

Supplementary Information

# Synergistic Effect of a Berlin Green Framework for Highly Efficient Moisture–Electric Energy Transformation

Minjae Song,‡[a] Daewoong Kim,‡[a] Hyewon Lee,[a] Hyunsoo Han[a] and Sangmin Jeon*[a]

[a]Department of Chemical Engineering, Pohang University of Science and Technology (POSTECH), 77 Cheongam-Ro, Pohang, Gyeongbuk, Republic of Korea

‡These authors contributed equally to this work.

* Author to whom correspondence should be addressed. E-mail: jeons@postech.ac.kr

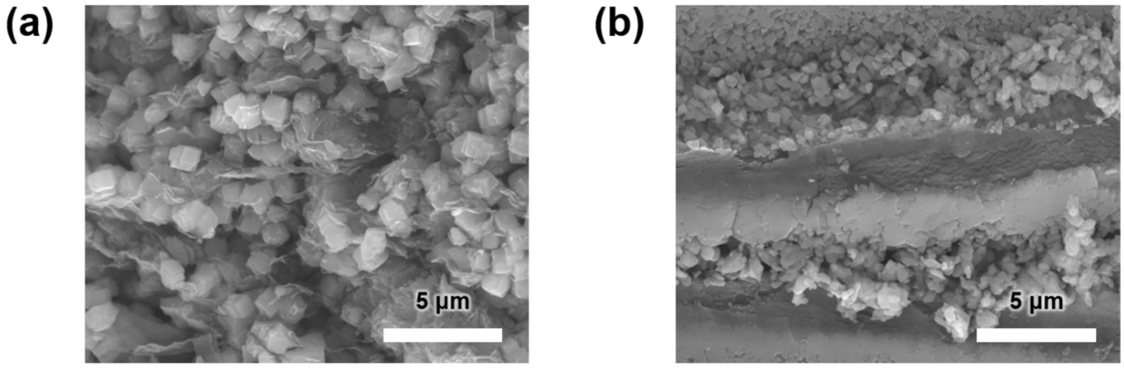


**Fig. S1.** SEM images of (a) BG particles in the BGC layer and (b) NaCl particles in the NC layer. NaCl and BG were incorporated in each layer in the form of crystalline particles, with sizes of ~1 μm (BG) and ~0.5 μm (NaCl).

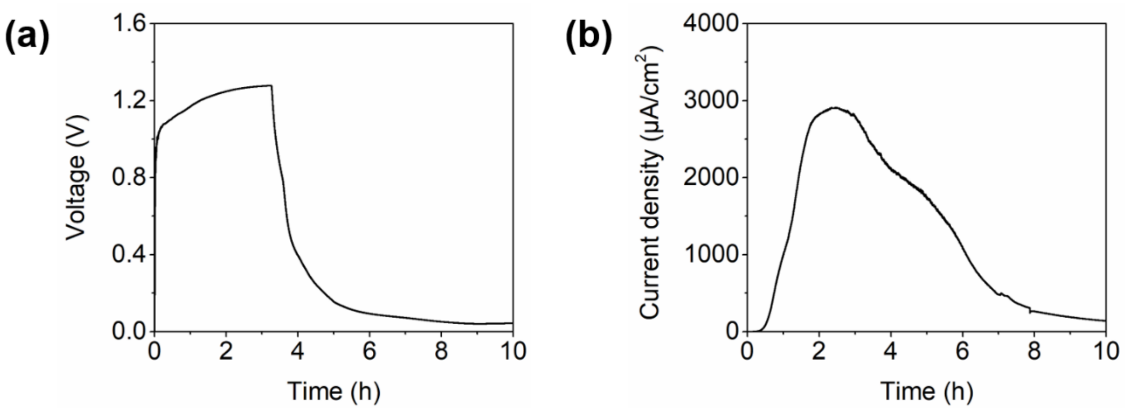


**Fig. S2.** Time-dependent changes in (a) open-circuit voltage and (b) short-circuit current density of BGC–NC at 90% RH for 10 h. Although the current density decreased from its peak value of 2,910 μA/cm$^2$, it sustained a level of 140 μA/cm$^2$ even after 10 h.

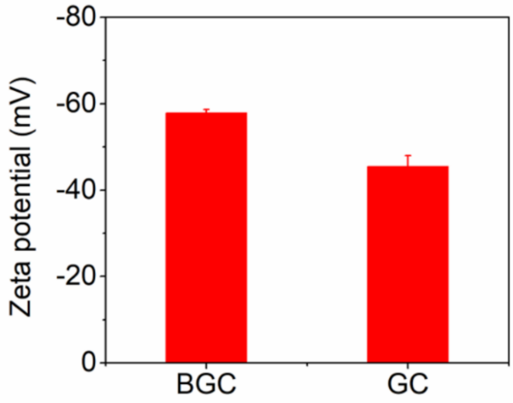


**Fig. S3.** Zeta potential of BGC and GC in DI water. Since BGC contains carboxyl and cyano functional groups, its surface becomes negatively charged at -57.8 mV.

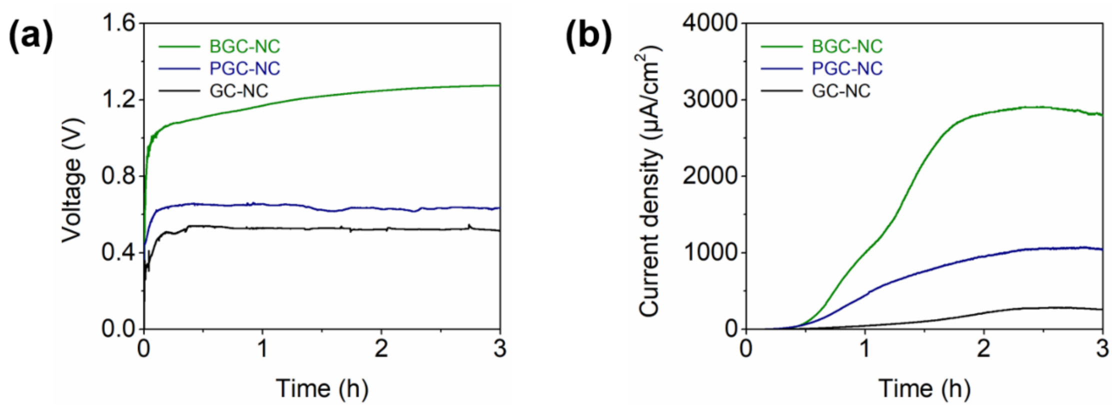


**Fig. S4.** Time-dependent changes in (a) voltage and (b) current density of GC–NC (black), PGC–NC (blue), and BGC–NC (green) at 90% RH for 3 h. The voltage (0.65 V) and current outputs (1,070 μA/$cm^2$) of PGC–NC were higher than those of GC–NC due to the increased surface area for the physical adsorption of $Na^+$ ions, but lower than those of BGC–NC.

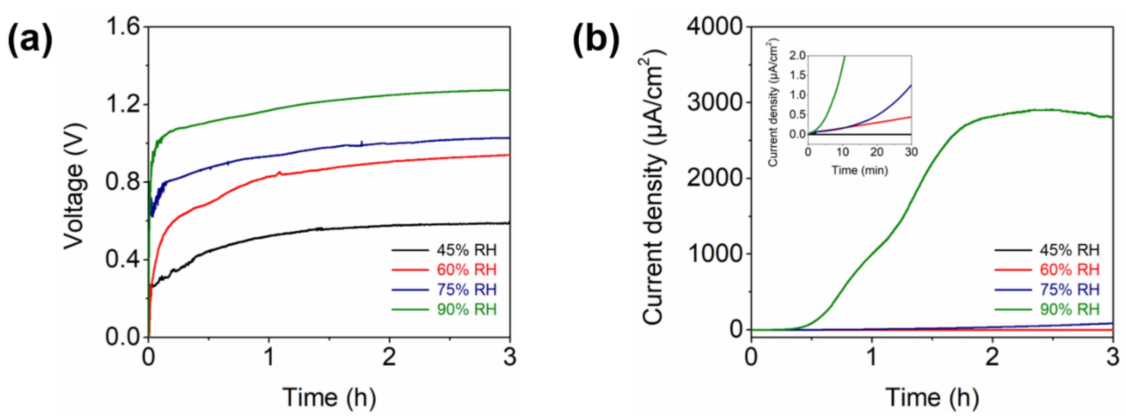


**Fig. S5.** Time-dependent changes in (a) voltage and (b) current density of BGC–NC at various RH values for 3 h. Inset provides a magnified view for below 75% RH. The voltage output increased with increasing RH, reaching its peak at 90% RH (1.28 V). Similarly, the current output increased with increasing RH, reaching 2,910 μA/cm$^2$ at 90% RH.

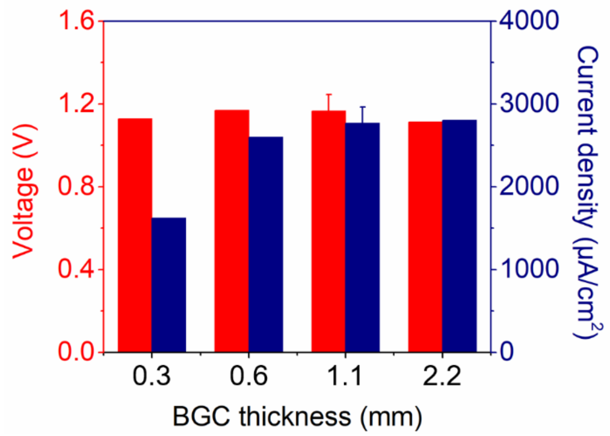


**Fig. S6.** Variations of the voltage (red) and current density (blue) output as a function of BGC layer thickness of BGC–NC. While keeping the thickness of the NC layer fixed at 0.2 mm, the thickness of the BGC layer was varied to 0.3, 0.6, 1.1, and 2.2 mm. The MEET performance increased as the BGC thickness increased, whereas it remained constant when the BGC layer thickness reached 2.2 mm.

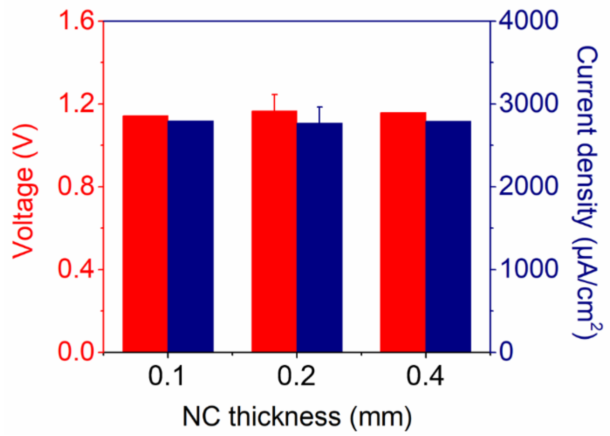


**Fig. S7.** Variations of the voltage (red) and current density (blue) output as a function of NC layer thickness of BGC–NC. While keeping the thickness of the BGC layer fixed at 1.1 mm, the thickness of the NC layer was varied to 0.1, 0.2, and 0.4 mm. The changes in the voltage and current outputs were negligible, indicating that the NC layer contains excess sodium ions that can reduce BG to PB.

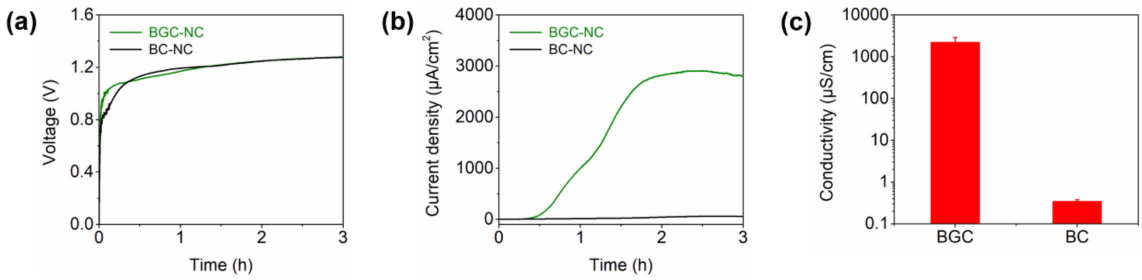


**Fig. S8.** Time-dependent changes in (a) voltage and (b) current density of BGC–NC (green) and BC–NC (black) at 90% RH for 3 h. (c) Electrical conductivity of BGC and BC. BC–NC reaches similar voltage (1.28 V), but has lower current and electrical conductivity (59.3 μA/cm$^2$, 0.347 μS/cm) compared to BGC–NC (2,910 μA/cm$^2$, 2,230 μS/cm), highlighting that GO acts as a conductive material within BGC.

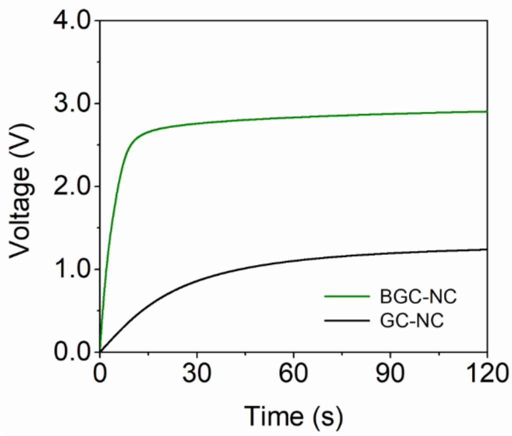


**Fig. S9.** Time-dependent changes in voltage when a 2000 μF capacitor is charged by three GC–NCs (black) or three BGC–NCs (green) at 90 % RH. When a 2000 μF capacitor was connected to three BGC-NCs, the BGC-NCs exhibited a much faster charging rate and reached a higher voltage than the GC-NCs.